Diversified and high elastic power grid planning method based on two-stage stochastic optimization

Hanyun Wang [1, *], Tao Wang [1], Hao Xu [2], Hongwei Mu [2] and Xiaoke Fan [2]

[1] Huzhou Power Supply Company of SGCC, Huzhou 313000, China.
[2] School of electrical and Electronic Engineering, North China Electric Power University, Beijing 102206, China.

Abstract. With the rapid development of distributed power generation, the study of multi-integrated and highly flexible grid planning methods has become a research hotspot. In multi-resource planning, the planning scheme that considers the active management mode is obviously better than the planning scheme that does not consider the active management mode. In this paper, a diversified and high elastic power grid planning method based on stochastic optimization is proposed, which can effectively deal with the impact of uncertainty caused by the access of distributed generation to the power grid, and provide a method support for the cleaning and efficiency of power system in the future. The IEEE 18 system example proves the feasibility and effectiveness of the proposed method.

Keywords: Distributed power; diversified and high elastic power grid; comprehensive evaluation.

1. Introduction

With the rapid development of smart grid technology, the diversified, integrated and highly resilient grid is based on a modern distribution network to achieve deep integration of information and communication technology and the planning, operation, control, and management of the distribution system, and a high proportion of consumption distribution It is a grid system with features such as green and low-carbon, safe and reliable, efficient interaction, smart openness, and balanced inclusiveness. It is a smart grid, An important part of the Energy Internet. This article summarizes the multiple fusion high-elasticity grid planning methods. Evaluation methods such as fuzzy comprehensive evaluation, ideal point approximation, grey correlation algorithm, entropy weight method [1], data envelopment and analytic hierarchy process are often used in comprehensive evaluation of power systems. The multi-convergence and highly resilient grid can achieve various operations through "source-source complementation", "source-network coordination", "network-load-storage interaction", and "source-network-load-storage coordinated optimization [2] “Energy interconnection and mutual benefit greatly improve the ability to optimize the allocation of energy resources in a wide area and the overall energy efficiency of the society. Diversified integration refers to distributed energy with increasing penetration levels in the distribution network, including distributed power generation, distributed energy storage, demand response, etc[5]. The multi-integrated and highly resilient grid can be attributed to the vertical integration of various elements of the source, network, load and storage, and the horizontal integration of the energy system, physical information, social economy, and natural environment. The multi-integrated high-elasticity grid has the function of resource optimization. It can form a strong receiving-end and sending-end power grid. It is an important power transmission and configuration platform in China. The country's overall investment, environmental protection, and energy production and utilization methods produce huge benefits [6].

2. The Planning Method of The Diversified and High Elastic Power Grid

2.1 Objective function

In order to promote the construction of a diversified and high elastic power grid, a certain number of distributed energy equipment and energy storage equipment will be considered in the process of grid expansion planning to enhance the economy and reliability of system operation. The consideration goal is to minimize the comprehensive cost of the power grid based on two-stage stochastic planning. The comprehensive cost is obtained by summing the investment cost of each stage of the construction decision and the operating cost of each stage during the planning period. Among them, the investment cost of the power grid comes from equipment investment, mainly from the cost of new construction and expansion of lines, distributed power sources such as wind power,

* Corresponding author: wanghanyun0204@sgcc.com.cn

photovoltaics, and equipment investment costs such as distributed energy storage; operating costs come from equipment operation and maintenance costs and conventional unit power generation Expenses, specifically, mainly include conventional unit power generation costs, distributed power operation and maintenance costs, energy storage operation and maintenance costs, network loss costs, load shedding costs, the objective function is expressed as:

$$\min F = \sum_{y \in Y} \frac{C_y^{INV} + C_y^{OPE}}{\left(1+\gamma\right)^Y} \tag{1}$$

Among them, F is the comprehensive cost during the system planning period, C_y^{INV} , C_y^{OPE} are the investment cost of the y-th stage and the operating cost of the y-th stage respectively, which are both phase index functions, γ is the discount rate, and Y is the length of the system planning cycle.

(1) Investment cost C_y^{INV}

$$\begin{aligned} C_y^{INV} = & \sum_{l \in \theta_{line\text{-}ET}} \sum_{k \in \Omega_{LM}} c_k^{line} x_{l,k,y}^{line\text{-}ET} l_k + \sum_{l \in \theta_{line\text{-}NC}} \sum_{k \in \Omega_{LM}} c_k^{line} x_{l,k,y}^{line\text{-}NC} l_k \\ & + \sum_{i \in \theta_{EES}} x_{i,y}^{EES} \left(c_P^{EES} \overline{P}_{i,y}^{EES} + c_E^{EES} \overline{E}_{i,y}^{EES} \right) \\ & + \sum_{i \in \theta_{WG}} x_{i,y}^{WG} c^{WG} \overline{P}_{i,y}^{WG} + \sum_{i \in \theta_{PV}} x_{i,y}^{PV} c^{PV} \overline{P}_{i,y}^{PV} \end{aligned} \tag{2}$$

Where, $x_{l,k,y}^{line\text{-}ET}$, $x_{l,k,y}^{line\text{-}NC}$, $x_{i,y}^{EES}$, $x_{i,y}^{WG}$, $x_{i,y}^{PV}$ Are the 0-1 decision variables of line reconstruction, line new construction, energy storage equipment, wind power, and photovoltaic in the y-th planning stage, c_k^{line} are the unit construction cost of the line (yuan/km), l_k are the line length (km), $\overline{P}_{i,y}^{EES}$ and $\overline{E}_{i,y}^{EES}$ are respectively the y-th The installed power c_P^{EES} and c_E^{EES} installed capacity (kW, kWh) of energy storage at node i in the planning stage,, c_P^{EES} are c_E^{EES} the unit power cost and unit capacity cost of energy storage (yuan/kW, yuan/kWh), respectively, $\overline{P}_{i,y}^{WG}$ and $\overline{P}_{i,y}^{PV}$ are the node i in the yth planning stage Installed wind power capacity and photovoltaic capacity (kW), c^{WG} are c^{PV} the unit capacity wind power installation cost and unit capacity photovoltaic installation cost (yuan/kW, yuan/kWh), respectively Ω_{LM} , $\theta_{line\text{-}ET}$, $\theta_{line\text{-}NC}$, θ_{EES} , θ_{WG} , θ_{PV} are the set of line models to be selected, and are to be retrofitted. Line set, line set to be newly built, node set to be selected for energy storage installation, node set to be selected for wind turbine installation, set of node to be selected photovoltaic installation.

(2) Operating cost C_y^{OPE}

$$\begin{aligned} C_y^{OPE} = & \phi \sum_{i \in \Omega_G} \sum_{s \in \Omega_S} \rho_s \sum_{t \in \Omega_T} \left[a_i \left(P_{i,t,s,y}^g \right)^2 + b_i P_{i,t,s,y}^g + c_i \right] \\ & + \phi c_{loss}^g \sum_{s \in \Omega_S} \rho_s \sum_{ij \in \Pi_{ij}} \sum_{t \in \Omega_T} I_{ij,t,s,y}^2 R_{ij,y} \Delta t \\ & + \phi c_{LC} \sum_{s \in \Omega_S} \rho_s \sum_{i \in \Pi_{node}} \sum_{t \in \Omega_T} P_{i,t,s,y}^{LC} \Delta t + \sum_{yy=1}^{y} \sum_{i \in \theta_{EES}} x_{i,yy}^{EES} c_{main}^{EES} \overline{P}_{i,yy}^{EES} \\ & + \sum_{yy=1}^{y} \left(\sum_{i \in \theta_{WG}} x_{i,yy}^{WG} c_{main}^{WG} \overline{P}_{i,yy}^{WG} + \sum_{i \in \theta_{PV}} x_{i,yy}^{PV} c_{main}^{PV} \overline{P}_{i,yy}^{PV} \right) - \beta E_{DG}^r \end{aligned} \tag{3}$$

Where ϕ is the typical number of days in stage y, ρ_s is the probability of scene s a_i , b_i , c_i are the energy consumption coefficients of conventional unit i (yuan/kW2, yuan/kW, yuan), and c_{loss}^g are the grid loss price per unit of electricity (yuan/ kWh), $P_{s,t,i,y}^g$ is the output (kW) of the conventional unit i in the y-th stage during the t period (kW), $I_{ij,s,t,y}$ is the power flowing through the line in the y-th stage (A), $R_{ij,y}$ is the line resistance in the y-th planning stage (Ω), Δt is the dispatching time, this paper takes 1h , c_{LC} is the unit load shedding cost (yuan/kWh), $P_{i,s,t,y}^{LC}$ is the load shedding power (kW), c_{main}^{EES} , c_{main}^{WG} , c_{main}^{PV} are the unit power maintenance cost of energy storage equipment (yuan/kW), wind turbine unit power maintenance cost (yuan/kW), Ω_S , Ω_T photovoltaic unit Power maintenance cost (RMB/kW), Π_{ij} , Π_{node} are the scene collection and scheduling time collection respectively, β are the system line collection and node collection respectively, are the subsidy cost per unit power generation of the renewable energy type RDG (ten thousand yuan/kWh), which E_{DG}^r are available RDG annual total power generation (kWh) of renewable energy types.

2.2 Constraints

(1) Line selection constraints

When optimizing the planning of the lines in the grid, in order to ensure the economic operation requirements of the system, at most only one line can be replaced or newly built at the same stage, so it can be expressed by line decision variables.

$$0 \le \sum_{k \in \Omega_{LM}} x_{l,k,y}^{line\text{-}ET} \le 1 \quad \forall l \in \left(\theta_{line\text{-}ET} \cup \theta_{line\text{-}NC} \right), \forall y \in Y \tag{4}$$

Where, $\left(\theta_{line\text{-}ET} \cup \theta_{line\text{-}NC} \right)$ Represents a collection of new lines to be selected and lines to be upgraded.

(2) Constraints on the number of distributed power installation nodes

$$0 \le \max_{y \in Y} \left(\sum_{i \in \theta_{WG}} x_{i,y}^{WG} \right) \le N^{WG} \tag{5}$$

$$0 \le \max_{y \in Y} \left(\sum_{i \in \theta_{PV}} x_{i,y}^{PV} \right) \le N^{PV} \tag{6}$$

Equations (15) and (16) respectively indicate that the number of nodes for installing wind power and photovoltaics in the system should be less than the allowable number of nodes, and, respectively N^{WG} , N^{PV} are the maximum number of nodes that can be installed with distributed power sources allowed by the system,, $\sum_{i \in \theta_{WG}} x_{i,y}^{WG}$, $\sum_{i \in \theta_{WG}} x_{i,y}^{PV}$ is the sum of the number of nodes installed in the system for wind power and photovoltaic power in the yth planning stage.

(3) Constraints on the number of installed nodes for energy storage equipment

There are also restrictions on the amount of energy storage in the system to ensure the minimum investment in the system.

$$0 \le \max_{y \in Y} \left(\sum_{i \in \theta_{EES}} x_{i,y}^{EES} \right) \le N^{EES} \tag{7}$$

Where N^{EES} is the maximum number of nodes that can be installed with energy storage devices allowed by the system, and $\sum_{i \in \theta_{EES}} x_{i,y}^{EES}$ is the sum of the number of nodes that can be installed with energy storage devices in the y-th planning stage.

(4) Distributed power installation capacity constraints

Since distributed power sources such as photovoltaics and wind power have strong intermittent and randomness, the safety and stability of the system must be ensured when the distributed power sources are connected. The installed power of the distributed power sources in the system must have a certain capacity limit [9]. Therefore, the following constraints are made:

$$0 \le \overline{P}_{i,y}^{WG} \le x_{i,y}^{WG} \overline{P}_{y}^{WG\text{-max}} \quad \forall i \in \theta_{WG}, \forall y \in Y \tag{8}$$

$$0 \le \sum_{i \in \theta_{WG}} \overline{P}_{i,y}^{WG} \le \max_{i \in \theta_{WG}} \left(x_{i,y}^{WG} \right) \overline{P}_{y}^{WG\text{-max}} \quad \forall y \in Y \tag{9}$$

$$0 \le \overline{P}_{i,y}^{PV} \le x_{i,y}^{PV} \overline{P}_{y}^{\text{PV-max}} \quad \forall i \in \theta_{WG}, \forall y \in Y \tag{10}$$

$$0 \le \sum_{i \in \theta_{PV}} \overline{P}_{i,y}^{PV} \le \max_{i \in \theta_{PV}} \left(x_{i,y}^{PV} \right) \overline{P}_{y}^{\text{PV-max}} \quad \forall y \in Y \tag{11}$$

Equations (18) and (19) respectively represent the upper limit of the installed power of wind power at a single node and the sum of all nodes in the y-th planning stage. Equations (20) and (21) respectively Indicates the upper limit of the installed power of the photovoltaic system at a single node and the sum of all nodes in the y-th planning stage. Where $\overline{P}_{y}^{WG\text{-max}}$, $\overline{P}_{y}^{PV\text{-max}}$ are the maximum wind power and maximum photovoltaic power (kW, kW) allowed to be installed in the system in the yth planning stage, and are the 0-1 variables used to judge whether there $\max_{i \in \theta_{WG}} \left(x_{i,y}^{WG} \right)$, $\max_{i \in \theta_{WG}} \left(x_{i,y}^{PV} \right)$ are wind turbines and photovoltaics installed in the system, respectively.

(5) Installation constraints on the capacity of energy storage equipment

In the current situation, the investment in energy storage equipment is expensive, so the installation of energy storage equipment in the system must also meet a certain capacity limit, so the constraint conditions such as equations (22) and 23) are made.

$$0 \le \overline{E}_{i,y}^{EES} \le x_{i,y}^{EES} \overline{E}_{y}^{EES\text{-max}} \quad \forall i \in \theta_{EES}, \forall y \in Y \tag{12}$$

$$0 \le \sum_{i \in \theta_{EES}} \overline{E}_{i,y}^{EES} \le \max_{i \in \theta_{EES}} \left(x_{i,y}^{EES} \right) \overline{E}_{y}^{EES\text{-max}} \tag{13}$$

Equation (12) is that the capacity of a single node in the yth planning stage meets the upper limit constraint, and equation (13) is that all the energy storage in the yth planning stage meets the upper limit constraint. $\overline{E}_{y}^{EES\text{-max}}$ is the upper limit (kWh) of energy storage allowed by the system.

(6) Output constraints of conventional units

The output of a thermal power unit cannot exceed the upper and lower limits of its own output in order to ensure its safe and stable operation. Therefore, there are the following constraints:

$$P_i^{g\text{-min}} \le P_{i,t,s,y}^{g} \le P_i^{g\text{-max}} \quad \forall i \in \Omega_G, \forall s \in \Omega_S, \forall t \in \Omega_T, \forall y \in Y \tag{14}$$

In the formula, and are respectively the upper limit and lower limit of output of thermal power unit i (kW, kW).

(7) Distributed energy output constraints

The output of distributed energy sources such as wind power and photovoltaics is related to real-time wind speed and light conditions, as shown in equations (15) and (17) respectively. Their output cannot exceed the maximum output limit at the current moment. (16) and formula (18).

$$P_{i,t,s,y}^{WG\max} = p_{s,t,y}^{WG} \sum_{yy=1}^{y} \overline{P}_{i,yy}^{WG} \tag{15}$$

$$0 \le P_{i,t,s,y}^{WG} \le P_{i,t,s,y}^{WG\max} \tag{16}$$

$$P_{i,t,s,y}^{PV\max} = p_{s,t,y}^{PV} \sum_{yy=1}^{y} \overline{P}_{i,yy}^{PV} \tag{17}$$

$$0 \le P_{i,t,s,y}^{PV} \le P_{i,t,s,y}^{PV\max} \tag{18}$$

Where $p_{s,t,y}^{WG}$ is the wind power coefficient, which $P_{i,t,s,y}^{WG\max}$ is a piecewise function of wind speed, $P_{i,t,s,y}^{WG}$ is the maximum wind power output (kW) at time t, $p_{s,t,y}^{PV}$ is the actual wind power output (kW) at time t, which does not exceed the maximum output range of wind power, $P_{i,t,s,y}^{PV\max}$ is the photovoltaic power coefficient , $P_{i,t,s,y}^{PV}$ is a function of light intensity, $P_{i,t,s,y}^{PV\max}$ is the maximum photovoltaic output (kW) at time t, $P_{i,t,s,y}^{PV}$ is the actual photovoltaic output (kW) at time t, which does not exceed the maximum output range of photovoltaics.

(8) Restrictions on charging and discharging of energy storage

The charge and discharge power of an energy storage device is affected by its installed power, and its charge and discharge power must also follow the capacity constraints [10].

$$0 \le P_{i,t,s,y}^{EES\text{-}C} \le \mu_{i,t,s,y}^{EES\text{-}C} \sum_{yy=1}^{y} \overline{P}_{i,yy}^{EES} \tag{19}$$
$$\forall s \in \Omega_S, \forall t \in \Omega_T, \forall i \in \theta_{EES}, \forall y \in Y$$

$$0 \le P_{i,t,s,y}^{EES\text{-dis}} \le \mu_{i,t,s,y}^{EES\text{-}dis} \sum_{yy=1}^{y} \overline{P}_{i,yy}^{EES} \tag{20}$$
$$\forall s \in \Omega_S, \forall t \in \Omega_T, \forall i \in \theta_{EES}, \forall y \in Y$$

$$0 \le \mu_{i,t,s,y}^{EES\text{-}C} \le 1 \quad \forall s \in \Omega_S, \forall t \in \Omega_T, \forall i \in \theta_{EES}, \forall y \in Y \tag{21}$$

$$0 \le \mu_{i,t,s,y}^{EES\text{-}dis} \le 1 \quad \forall s \in \Omega_S, \forall t \in \Omega_T, \forall i \in \theta_{EES}, \forall y \in Y \tag{22}$$

$$0 \le \mu_{i,t,s,y}^{EES\text{-}dis} + \mu_{i,t,s,y}^{EES\text{-C}} \le 1 \tag{23}$$
$$\forall s \in \Omega_S, \forall t \in \Omega_T, \forall i \in \theta_{EES}, \forall y \in Y$$

Formulas (19) and (20) are the charging power constraint and discharging power constraint of energy storage equipment respectively, and the charging and discharging power cannot exceed the installed power of the energy storage. Formulas (21)-(23) is to constrain the energy storage charging and discharging signs to ensure that only one state can be in progress at the same time. In the formula, $P_{i,t,s,y}^{EES\text{-}C}$, $P_{i,t,s,y}^{EES\text{-dis}}$ are the charging power and discharging power (kW, kW) of the energy storage device of section i at time t, respectively, $\mu_{i,t,s,y}^{EES\text{-C}}$, $\mu_{i,t,s,y}^{EES\text{-}dis}$ are the symbols indicating the charging and discharging status of the energy storage, when it is 0, it means not charging or discharging, which is 1 o'clock indicates that the energy storage is charging and discharging.

(9) Constraints on remaining energy of energy storage

The life of the energy storage device is generally related to the depth of charge and discharge. Overcharge and overdischarge will increase the life loss of the energy storage device. Therefore, the remaining capacity and state of charge of the energy storage device at time t need to be restricted:

$$SOC_{\min} \sum_{yy=1}^{y} \overline{E}_{i,yy}^{EES} \le E_{i,t,s,y}^{EES} \le SOC_{\max} \sum_{yy=1}^{y} \overline{E}_{i,yy}^{EES} \tag{24}$$
$$\forall s \in \Omega_S, \forall t \in \Omega_T, \forall i \in \theta_{EES}, \forall y \in Y$$

$$E_{i,t,s,y}^{EES} = E_{i,t\text{-}1,s,y}^{EES} + \left(P_{i,t,s,y}^{EES\text{-}C} \eta_C - \frac{P_{i,t,s,y}^{EES\text{-dis}}}{\eta_d} \right) \Delta t \tag{25}$$
$$\forall s \in \Omega_S, \forall t \in \Omega_T, \forall i \in \theta_{EES}, \forall y \in Y$$

$$E_{i,T,s,y}^{EES} = E_{i,0,s,y}^{EES} \quad \forall s \in \Omega_S, \forall t \in \Omega_T, \forall i \in \theta_{EES}, \forall y \in Y \tag{26}$$

Equation (24) represents the system SOC constraint, the remaining power of energy storage cannot exceed its upper and lower limits, Equation (25) represents the energy storage power balance constraint, and Equation (26) represents the energy storage beginning and ending power constraints to ensure storage The remaining power of the device at the beginning of a cycle is equal to the remaining power at the ending time. Where $E_{i,t,s,y}^{EES}$ is the remaining power (kWh) at time t of the energy storage, and, $SOC_{\max}$, $SOC_{\min}$ respectively represent the maximum and minimum state of charge of the energy storage device, η_C represent the charging efficiency of the energy storage, represent the discharge efficiency of the energy storage, and $E_{i,0,s,y}^{EES}$ represent the remaining energy storage at the initial time Electricity (kWh).

(10) Loss of load restraint

The load loss of the system node cannot exceed the original load of the node

$$0 \le P_{i,t,s,y}^{LC} \le P_{i,t,s,y}^{L} \quad \forall s \in \Omega_S, \forall t \in \Omega_T, \forall i \in \Pi_{node}, \forall y \in Y \tag{27}$$

Where $P_{i,s,t,y}^{L}$ is the load of the system node i at time t.

(11) Power balance constraints

In the coordinated planning of the distribution network and distributed energy, the safe and stable operation of the system must also be ensured, and active power balance

and reactive power balance must be met at each node, as shown below:

$$\sum_{i\in j}\left(P_{ij,t,s,y}^{line}-I_{ij,t,s,y}R_{ij,y}\right)+P_{i,t,s,y}^{g}+P_{i,t,s,y}^{WG}+P_{i,t,s,y}^{PV}+P_{i,t,s,y}^{EES\text{-dis}} =\sum_{k\in j}P_{jk,t,s,y}^{line}+P_{i,t,s,y}^{EES\text{-}C}+\left(P_{i,t,s,y}^{L}-P_{i,t,s,y}^{LC}\right) \quad (28)$$

$$\sum_{i\in j}\left(Q_{ij,t,s,y}^{line}-I_{ij,t,s,y}X_{ij,y}\right)+P_{i,t,s,y}^{g}\tan\alpha^{g}+P_{i,t,s,y}^{WG}\tan\alpha^{WG}+P_{i,t,s,y}^{PV}\tan\alpha^{PV} =\sum_{k\in j}Q_{jk,t,s,y}^{line}+\left(Q_{i,t,s,y}^{L}-P_{i,t,s,y}^{LC}\frac{Q_{i,t,s,y}^{L}}{P_{i,t,s,y}^{L}}\right) \quad (29)$$

Where, $P_{i,t,s,y}^{L}$, $Q_{i,t,s,y}^{L}$ are the active load and reactive load (kW, kVar) of node i, $P_{ij,t,s,y}^{line}$, $Q_{ij,t,s,y}^{line}$ are the active power and reactive power (kW, kVar) that flow through the head end of line ij in time period t, α^{g} , α^{WG} , α^{PV} are respectively The power factor angle of conventional units, wind turbines and photovoltaics.

3. Case Study

3.1 Example of 18-bus power distribution system

A regional power distribution system in Huzhou, Zhejiang Province is selected as an example to verify the effectiveness of the proposed method. The network has 10 nodes and 9 lines in the initial year. In the future, it will increase to 18 nodes. The network topology is shown in Figure 1.

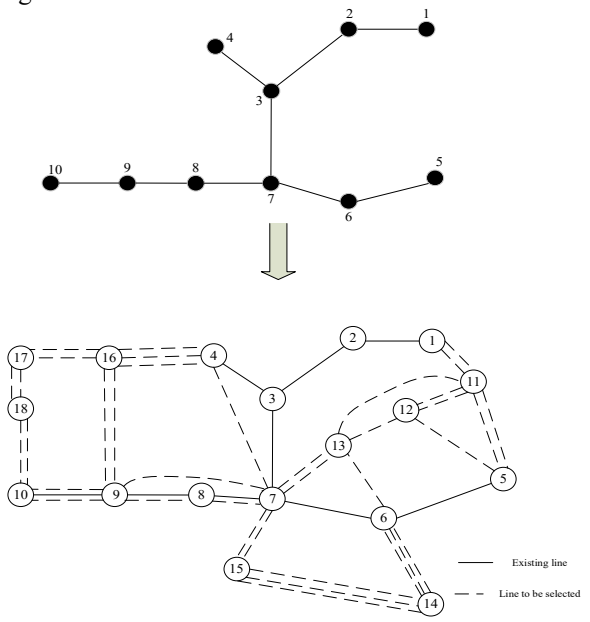

Figure 1. 18-node distribution network structure diagram

3.2 Analysis of random planning results

The distribution network planning research is carried out for the calculation examples in the following three situations:

Scenario 1: Traditional distribution network planning without RDG;

Scenario 2: Consider the traditional distribution network planning of RDG access;

Scenario 3: Consider RDG access to the uncertain distribution network planning, and carry out random planning;

When the genetic algorithm finds the optimal solution, the initial population size is 100, the crossover probability is 0.8, the redistribution probability is set to 0.2, and the termination algebra T=100. The optimal value does not change for 70 times, which is convergence.

The area to be planned shall be planned according to the traditional distribution network planning without considering DG and RDG access, and the random planning considering the integration and interaction of multiple resources. The planning results are shown in Figure 2, 3, and 4 and Table 1:

Table 1. Planning results

plan	Optimize route information	RDG access		
		Wind Turbines	Photovoltaic generator	Energy storage device
Traditional distribution network planning without RDG	1-11, 4-16, 5-12, 6-14(2), 7-8, 7-13, 8-9, 9-10(2), 14-15, 16-17(2), 17-18	/	/	/
Traditional distribution network planning considering RDG access	1-11(2), 4-16(3), 6-14(2), 7-8, 7-13(2), 8-9, 9-10(2), 14-15, 16-17(2), 17-18	4(2), 8(2), 17(4), 18(3)	5(3), 11(2), 12(2), 13(1), 15(3)	4(1), 5(1), 10(1), 11(2), 12(2), 15(2), 17(2), 18(2)
Two-stage stochastic planning	1-11, 4-16(2), 6-14(2), 7-8, 7-13, 7-15, 8-9, 9-10(2), 10-18, 11-12(2), 14-15, 16-17(2)	4(3), 10(3), 17(5), 18(6)	5(2), 11(2), 12(3), 14(3), 15(4)	4(2), 5(1), 10(1), 11(2), 12(2), 14(2), 15(2), 16(1), 17(4), 18(4)

Note: In the planning scheme, "5(3)" means 5 nodes to install 3 corresponding RDGs, and "/" means not to install.

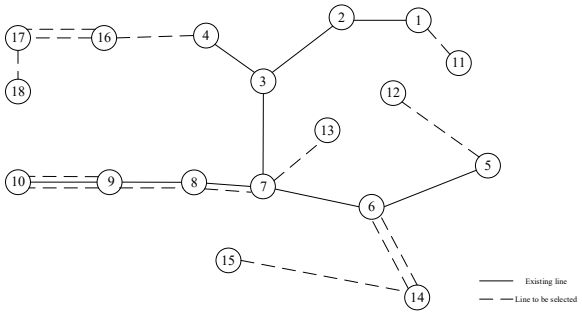

Figure 2. Traditional distribution network planning scheme without RDG

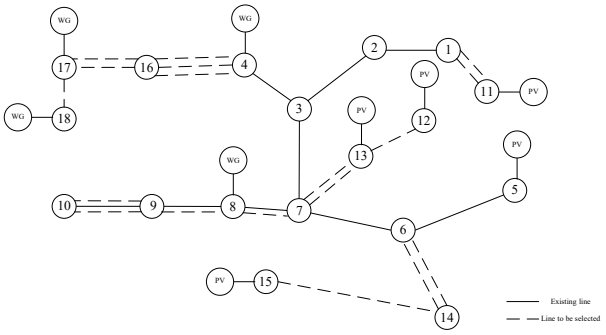

Figure 3. Traditional distribution network planning scheme considering RDG access

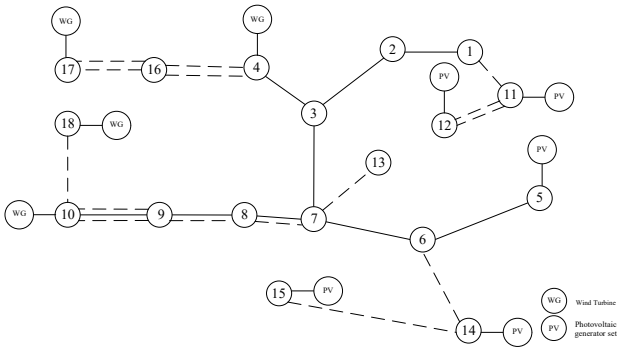

Figure 4. Random planning scheme of distribution network considering RDG access

The costs of the three programs are shown in Table 2.

Table 2. The cost of each planning scheme

Cost (ten thousand yuan)	Scenario 1 Traditional distribution network planning without RDG	Scenario 2 Traditional distribution network planning considering RDG access	Scenario 3 Two-stage stochastic planning considering RDG access
Line investment annual fee	390.22	201.41	189.82
RDG and energy storage investment costs	/	1312.30	1886.50
Power purchase cost of superior grid	13279.63	11651.85	10931.93
RDG and energy storage maintenance costs	/	883.80	910.97
Network loss cost	62.23	55.11	50.99
Environmental protection subsidy	/	436.80	643.02
Comprehensive grid cost	13732.08	13667.67	13327.19

From the data in the table, it can be seen that Scenario 1 is a distribution network planning solution that does not consider RDG, Scenario 2 is a traditional distribution network planning solution that considers RDG access, and Scenario 3 is a two-stage stochastic planning solution that considers RDG access. The data can be derived:

1) The annual network investment cost of Scenario 1 is 1.8881 million yuan more than that of Scenario 2 and 2.004 million yuan more than that of Scenario 3. This is because after joining RDG, it can bear part of the load and reduce the investment in the upgrade and construction of the power distribution system, regardless of RDG planning. In the plan, because there is no RDG to bear the load, it is necessary to increase the network investment of the distribution system; and the network investment cost of the plan 2 is 6.11% more than that of the plan 3. This shows that the two-stage stochastic planning plan considering RDG access can better improve the system The ability to accept RDG, and the joint planning of RDG and network can make RDG more reasonable access to the distribution network, and make the grid structure more suitable for RDG access.

2) In the comparison of network loss costs, Scenario 3 is 509,000 yuan, which is 18.1% less than Scenario 1, and 7.48% less than Scenario 2. This is because the two-stage stochastic planning solution considering RDG access can be better utilized RDG plays a positive role in reducing system network loss and improving system operation.

3) In the comparison of the power purchase cost of the higher-level power grid, Scenario 3 is 109.3193 million yuan, which is 23.477 million yuan less than Scenario 1, and 7.199.2 million yuan less than Scenario 2. This is due to the two-stage stochastic planning plan considering RDG access. RDG generates more power and bears a larger load, so it purchases less electricity from the upper-level grid; in Scenario 2, because RDG is not actively managed, the distribution network's ability to accept RDG output is smaller than that in Scenario 3. Therefore, the RDG's power generation is relatively small, and the power purchase from the upper-level grid is relatively large; similarly, since the influence of RDG is not considered in Scenario 1, all loads in the system must be borne by the substation, so this solution The purchase of electricity from the upper-level grid is the largest.

4. Conclusion

In this paper, a two-stage stochastic planning model of the diversified and high elastic power grid was proposed, and the joint planning result of the distribution network with distributed power generation under the multi-integration and high flexibility was obtained. The conclusion is as below:

Distributed power generation planning and distribution network framework planning are a whole that influences and cooperates with each other. Joint modeling and solving of them can conform to the development trend of active distribution network with large-scale distributed power generation in the future. At the same time, from the perspective of social comprehensive cost, the random planning scheme considering RDG access is the best, which proves that the multi-integrated and highly flexible distribution network can overcome the shortcomings of

DG's "install and forget" management principle, and rationally integrate RDG to make RDG Actively participating in the optimization of the operation of the distribution network will help improve the system's ability to accept renewable energy, promote the development of RDG, and make the system cleaner and more efficient.

Acknowledgments

The study is funded by Huzhou Power Supply Company of SGCC (Research on theoretical framework of diversified and high elastic power grid, SGZJHU00FZJS2000611).

References

1. Research on optimal configuration of multi-energy complementary combined supply system based on entropy weight-TOPSIS Zhang Dong1,2 Zhang Bin1,2 Zhang Rui1,2 An Zhou Jian1 Journal of Huazhong University of Science and Technology (Natural Science Edition)
2. Shuai Wanlan, Zhu Ziwei, Li Xuemeng, Luo Zhijiang, Zhu Hailong, Zhang Yining. Integrated energy system "source-grid-load-storage" collaborative optimization operation considering wind power consumption[J]. Power system protection and control, 2021, 49(19):18-26.
3. Yin Jijun, Xia Qing. Conceptual design and exploration of multi-integrated high-resilient power grid in the form of energy Internet[J]. Proceedings of the Chinese Society of Electrical Engineering, 2021, 41(02): 486-497.
4. Hang Haiyan, Yang Liqiang, Gan Wen, Sun Yi, Yang Hongyue, Li Zekun. Multi-time scale optimal dispatch strategy considering demand response in highly elastic power grid[J]. Journal of North China Electric Power University (Natural Science Edition), 2021, 48(04): 40-48.
5. Zhou Bingkai, Yang Xiaofeng, Li Jicheng, Nong Renbiao, Chen Qian. Overview of key technologies for multi-integrated and highly resilient power grids [J]. Zhejiang Electric Power, 2020, 39(12): 35-43.
6. Yin Jijun. Building an energy Internet to empower a beautiful China-Promoting the high-quality development of energy through the construction of a multi-integrated and highly flexible power grid [J]. Contemporary Electric Power Culture, 2021(02): 34-37.
7. Feng Changsen, Zhang Yu, Wen Fushuan, Ye Chengjin, Zhang Youbing. Microgrid energy management strategy based on deep expectation Q network algorithm [J/OL]. Power system automation: 1-17 [2021-10-29].
8. Zhu Lan, Liu Shen, Tang Longjun, Wang Ji, Huang Chao. Uncertainty response modeling of charge and discharge and day-ahead scheduling strategy of electric vehicle agents[J]. Power System Technology, 2018, 42(10): 3305-3317.
9. Liu Zhiwen, Dong Xuzhu, Huang Yu, Wu Zhengrong. Calculation method of the maximum penetration rate of distributed power considering multiple constraints[J]. Journal of Electric Power System and Automation, 2019, 31(06): 85-92.
10. Bai Xueting, Yang Ruiqi, Chen Zechun, Yang Dechang. Optimal operation of the park's integrated energy system considering the comprehensive demand response[J]. Journal of Electric Power Science and Technology, 2021, 36(03): 27-35.